Electronic excitation in impact scattering of low-energy He^+ from solid surfaces

R. Souda, T. Aizawa, C. Oshima, S. Otani, and Y. Ishizawa
National Institute for Research in Inorganic Materials, 1-1 Namiki, Tsukuba, Ibaraki 305, Japan
(Received 12 December 1988)

Inelastic scattering and electron-exchange processes in low-energy (0.1–1 keV) He^+ scattering from surfaces of ionic compounds and metallic elements have been investigated. The probability for ionization of neutral He^0 in the ground state is minimized for target elements which have filled *d* orbitals located in a shallower energy position than the He 1*s* level. Inelastic scattering other than reionization of He^0 is also clearly observed in the spectra from a large number of ionic compounds. These excitations are observed provided that the surface *p* levels are located at lower energies than the He 1*s* level and that ionization of He^0 takes place with a large probability. On the basis of the quasimolecular framework, it is found that the inelastic scattering is caused by excitation of surface *p* electrons along the σ orbital, which is promoted due to the antibonding interaction with the He 1*s* orbital. The quantum-mechanical interference between bonding and antibonding orbitals, which results in oscillatory-yield–versus–kinetic-energy curves because of the quasiresonant charge exchange, is found to be broken down by the intervening occurrence of the inelastic process.

I. INTRODUCTION

Since an early work by Smith,[1] low-energy ion-scattering spectroscopy (ISS) using rare-gas ions has been applied for analyzing the composition and the structure of solid surfaces.[1–3] The ions reflected from the bulk are neutralized with such a large probability that the ions scattered from the outermost surface layer are selectively detected without neutralization[4,5] The ion scattered into a laboratory scattering angle θ_L, therefore, is expected to have a kinetic energy E_1 corresponding to single binary collision given by the following well-known equation:

$$E_1 = E_0[M_0/(M_0+M)]^2 \times \{\cos\theta_L + [(M/M_0)^2 - \sin^2\theta_L]^{1/2}\}^2 , \quad (1)$$

where E_0 and M_0 are the primary kinetic energy and the mass of the projectile ion, respectively, M being the mass of the target atom. In investigating ISS spectra from various surfaces, however, it has become apparent that the spectral peak usually deviates from the energy position expected from Eq. (1),[6–8] and is often accompanied by satellite peaks which should be ascribed to multiple scattering or a certain inelastic process.[9–12] The multiple-scattering effect can easily be identified by changing the scattering geometry and is minimized under the condition of impact scattering.[13]

The inelastic scattering of the rare-gas ions from solid surfaces is one of the most fundamental processes of the particle-surface interaction and has recently attracted much attention since its mechanism has not completely been clarified yet. The inelastic ion scattering due to electronic excitation may probably be classified into the two processes shown in Fig. 1: One is charge-exchange excitation (CEE), which is accompanied by the electron exchange between projectiles and solid surfaces, and the other is collision-induced excitation (CIE) of surface electrons, in which the charged state of the ions are conserved before and after the collision. Among the CEE processes, neutralization due to the Auger process (AN), as well as the resonance process,[14,15] which includes the valence-band resonance process (RN) and the quasiresonant charge-exchange process (QRN), causes very little change in the kinetic energy E_0 of the projectile, while (re)ionization, in which an electron of the neutralized projectile is transferred to a vacant valence level of a surface, is of essential importance since the (re)ionized neutral loses a large energy ΔE comparable to the ionization energy of the projectile, and therefore is frequently responsible for the loss peak in the ISS spectra.[16–18] The excitation of surface valence electrons is thought to be inevitable in ion scattering from solid surfaces and appears as a shift of the binary-collision peak towards a lower-energy position than expected from Eq. (1).

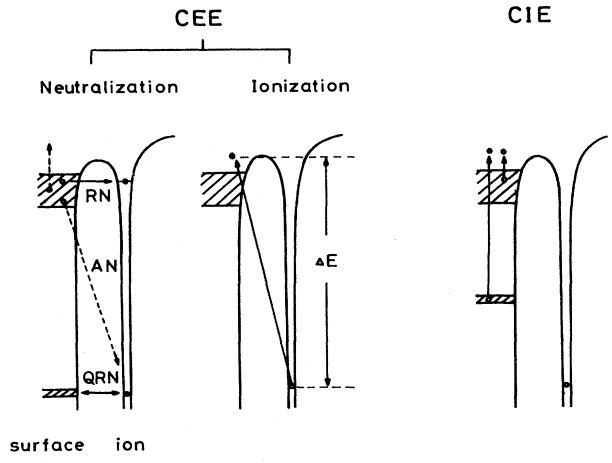

FIG. 1. Possible mechanism of inelastic ion scattering due to electronic excitation.

The scattered-ion spectra, therefore, is at least composed of two components; one comes from the ions surviving neutralization, which consist of the elastically scattered ions as well as the ions scattered inelastically after exciting valence electrons, and the other is reionized neutral atoms, which where once neutralized due to the Auger process in their incoming trajectory, then reionized in the violent collision, and finally survived neutralization in their outgoing trajectory.[16] Of physical interest is the influence of the surface-electronic structure on these inelastic processes. Reionization is essentially considered to be a diatomic process in which the electron-transfer probability is dependent on the ion-target combination,[16–20] but is pointed out to be influenced by the electronic band structure of a surface.[21,22] Ion neutralization is also known to be affected by the chemical environment of a target atom.[23] For example, the neutralization probability of He^+ increases remarkably due to oxidation of the metallic surfaces, such as Ta or TiC(111), while the loss peak that may be ascribed to reionization is relatively enhanced due to oxidation.[12,23] The inelastic He^+ scattering caused by excitation of valence electrons is necessarily affected by the electronic states of the target materials.

The effect of surface-electronic structure on the inelastic ion scattering, which we call the band effect, is essential for obtaining information on the mechanism of the electronic transition during ion scattering and has been investigated by comparing the He^+ spectrum for a certain target atom in elemental form with that in compound form.[24] In this paper we demonstrate that the band effect plays an important role in various aspects of the charge-exchange process and the inelastic process of low-energy (0.1–1 keV) He^+ ions scattered from solid surfaces. It will be claimed that the promotion of the He 1*s* orbital in the quasimolecular (QM) state, which has been estimated from the ionization probability of neutral He atoms, is strongly suppressed if the target atoms have filled *d* orbitals located in the shallower energy position than the He 1*s* orbital, and that the excitation of the surface *p* electrons to the conduction band takes place with a large probability provided the He 1*s* orbital is promoted enough in the QM state.

II. EXPERIMENT

Figure 2 shows a schematic of our experimental apparatus. The ISS spectra can be taken using beams of He^+ ions and neutral He atoms in the ground state, He^0, with kinetic energy ranging from 0.1 to 1 keV. A He^+ beam is produced by a discharge-type ion source and is mass-analyzed by a Wien filter, while a He^0 beam is produced by passing a He^+ beam through a charge-exchange cell in which a He gas is introduced up to 1×10^{-5} Torr, the conversion efficiency of He^+ to He^0 ranging from $\sim10\%$ (100 eV) to $\sim30\%$ (1000 eV). The energy spread of the He^+ beam is kept below 1.5 eV during the measurements and can be minimized to 0.5 eV by optimizing the discharge condition of the ion source. The He^+ and He^0 beams were incident upon a surface with a certain glancing angle α, and the He^+ ions, together with secondary ions scattered at θ_L with respect to primary-beam directions, are detected by using a hemispherical electrostatic analyzer operating with an energy resolution of 1 eV. The experimental chamber is evacuated down to ultrahigh-vacuum (UHV) conditions (3×10^{-11} Torr in base pressure) and is equipped with facilities for sample preparation and characterization such as differentially pumped sample evaporators, a sample-heating system, a sputter-etching ion gun, electron guns for low-energy electron diffraction (LEED) as well as electron-energy-loss spectroscopy (EELS), and x-ray and ultraviolet sources for photoelectron spectroscopy.

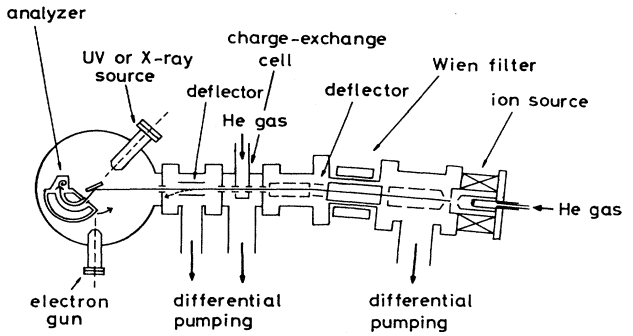

FIG. 2. Schematic of an experimental apparatus used for ISS in which not only He^+ but also He^0 is used as a primary beam. The He^+ beam is extracted from a discharge-type ion source in which a coaxial magnetic field can be applied in cases for obtaining a high beam current, and is then mass-analyzed by a Wien filter and deflected at 3° to eliminate a fast neutral beam produced at the ion source. After deceleration by means of electrostatic lenses, a He^+ beam is introduced into a charge-exchange cell in which a neutral He^0 beam with the same kinetic energy as a primary He^+ beam can be produced due to resonance charge exchange of a He^+-He system. A pure He^0 beam is then produced by eliminating residual He^+ by using an electrostatic deflector at the entrance to the experimental chamber.

In the present work, experiments were made for the following 39 samples with a form of pure elements such as Na, Mg, K, Ca, Mn, Co, Ni, Cu, Zn, Ga, Ge, Ag, Cd, In, Sn, Sb, Te, Au, and Pb, together with compounds such as NaCl, MgF_2, KBr, KI, CaF_2, TiC, CuCl, $ZnCl_2$, RbCl, $SrCl_2$, SrF_2, MoO_3, AgCl, $SnCl_2$, CsCl, $BaCl_2$, PrF_3, LuF_3, TaC, and HfC. Most of the samples were polycrystals prepared by deposition in UHV on a substrate of graphite in thermal evaporation, but several of them were single crystals (TiC, CaF_2, NaCl, KBr, etc.). The single-crystal surfaces of ionic compounds were prepared by cleavage in air and heating in UHV for cleaning and annealing, and exhibited a sharp 1×1 LEED pattern. All samples thus prepared showed no oxygen contamination in the preliminary ISS measurements. Charging effects for insulating samples were successfully resolved by heating them up to 300 °C. Some of the metallic samples were also exposed to O_2 and Cl_2 gases, which were introduced into the sample chamber in a dynamical-flow mode so as to keep the pressure below 1×10^{-6} Torr.

III. EXPERIMENTAL RESULTS

A. Ionization of He^0

The He^+ ions scattered from solid surfaces are neutralized due to the Auger process ($He^+ \rightarrow He^0$) with a probability dependent on the scattering trajectory. The resultant He^0 can partly be reionized in the collision with a target atom. Reionization of He^0 sometimes makes a dominant contribution to the He^+ spectra at such a low kinetic energy below 1 keV,[16] and its occurrence is known to be essential for the surface-structure analysis by ISS (Refs. 18 and 25) or the appearance of multiple scattering in the ISS spectra.[17]

(Re)ionization of He^0 is thought to be caused by promotion of a He 1s electron with a binding energy of 24.6 eV to a vacant valence level of the surface, so that its probability is a good method for probing the behavior of molecular orbitals in the QM state. We have chosen the He^+ intensity by He^0 incidence relative to that by He^+ incidence, I^0/I^+, as a measure of the promotion of the He 1s orbital, the beam intensities of both He^+ and He^0 being normalized relative to each other via secondary-ion yields.[26] The values for the 22 target elements in the Periodic Table at a kinetic energy of 1 keV are shown in Fig. 3. It is found that the values have a steep minimum for the group-IIb elements and a maximum around the alkaline-earth elements for both fourth- and fifth-row elements; it should be noted that the value for Zn or Cd is about 3 orders of magnitude smaller than that for Ca.

As regards electronic excitation in a violent atomic collision, the diabatic correlation diagram (DCD) proposed by Barat and Lichten[27] is known to be effective for investigating the core-electron excitation in asymmetric diatomic scattering. However, the experimental result that the I^0/I^+ values for the fifth-row elements show a steep minimum around the group-IIb elements apparently contradicts the theoretical prediction based on DCD, since, according to DCD, the He 1s orbital should be sufficiently promoted in the QM state formed with all of the fifth-row elements. On the other hand, the molecular-orbital calculation that is consistent with our experimental results has recently been made by Tsuneyuki and Tsukada.[20] They conclude that the promotion of the He 1s orbital is caused by the interaction with a core orbital of the target atoms.

As shown in Fig. 3, the ionization probability of He^0 seems to be suppressed as the number of d electrons increases, and it jumps for the group-IIIb elements. The d orbitals of the group-IIIb elements such as Ga and In are located energetically so favorable for the quasiresonant charge exchange with the He 1s orbital that the scattered-ion yield shows well-known oscillations against the kinetic energy.[15] As will be discussed later, promotion of the molecular orbitals formed by mixing of these atomic orbitals is responsible for quasiresonant charge exchange as well as excitation of the He 1s electron. The occupied d levels of the group-IIIb elements, however, are located at so shallow an energy position compared with the He 1s level that mixing of the two atomic orbitals is expected to be very small. This may offer a reason

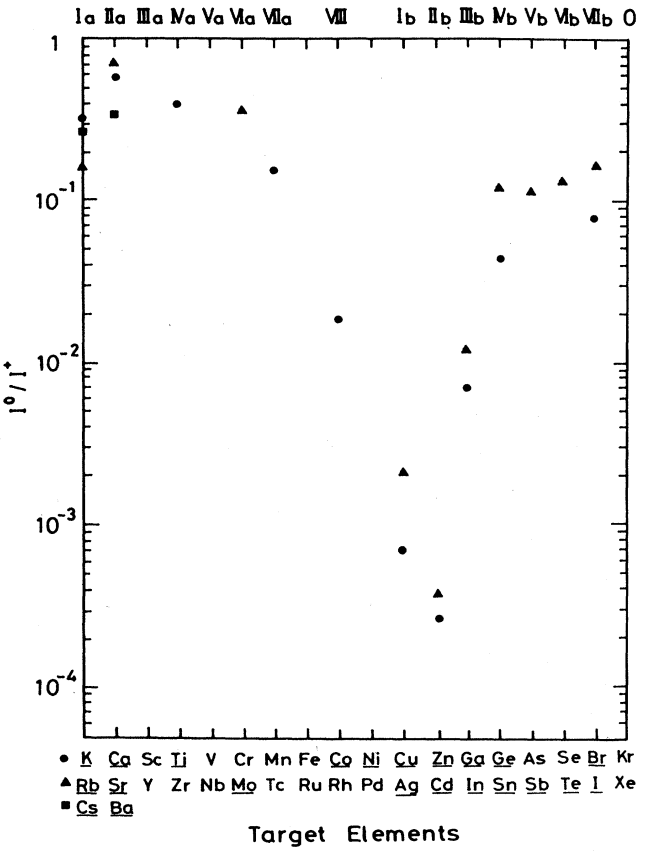

FIG. 3. The ionization probability of He^0 for 22 target elements estimated from the normalized He^+ intensity by He^0 incidence to that by He^+ incidence, I^0/I^+, at a kinetic energy of 1 keV obtained under the scattering geometry of $\alpha = 80°$ and $\theta_L = 160°$.

why there exists a large gap in the ionization probabilities between the group-IIb elements and the group-IIIb elements. It is thus concluded that, in the kinetic-energy region below 1 keV, the promotion of the He 1s electron is strongly suppressed if the target atom has filled d levels located in an energy position shallower than the He 1s level. It should be noted that the ionization probability generally increases with increasing the kinetic energy, and even the target elements with a very small I^0/I^+ value shown in Fig. 3 can yield ionization of He^0 with a large probability if the kinetic energy reaches several keV.[28]

B. Excitation of valence electrons

1. *Sr, SrF_2 (111)*

Figure 4 shows energy spectra of He^+ obtained by using an $E_0 = 200$ eV He^+ beam from (a) a pure Sr surface and Sr surfaces exposed to (b) 100 L O_2 and (c) 10 L Cl_2 (1 L = 1 langmuir $\equiv 10^{-6}$ Torr s), together with the He^+ spectra obtained by using an $E_0 = 200$ eV He^0 beam as in-

dicated by dotted curves, the glancing angle α and the scattering angle θ_L being fixed at 80° and 160°, respectively. The spectra for He^+ and He^0 incidence are normalized relative to each other by a calibration of the beam intensities. The Sr peak from the metallic surface is about 10 eV full width at half maximum (FWHM), with a deviation of about 4 eV from the ideal binding collision energy (BCE) indicated by arrows on the abscissa ($E_1 = 167.5$ eV). The low-energy tail, corresponding well to the ionized He^0 spectrum appearing in the energy position about 21 eV below the BCE, is considered attributable to reionization.

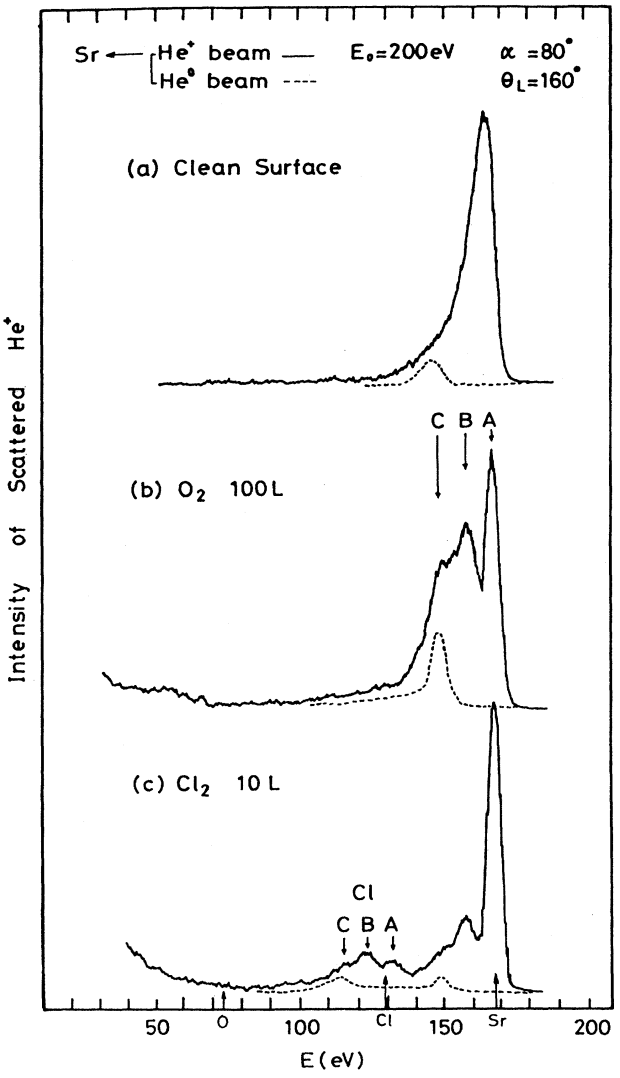

FIG. 4. Energy spectra of He^+ from (a) a clean Sr surface and the Sr surface exposed to (b) 100 L O_2 and (c) 10 L Cl_2 obtained by using a He^+ beam and a He^0 beam with a kinetic energy of 200 eV. The spectrum obtained by He^0 incidence (dotted curve) is normalized to that by He^+ incidence (solid curve) by calibrating beam currents via secondary-ion yields. A binary collision energy (BCE) for each element is indicated by arrows on the abscissa.

If the metallic surface is exposed to oxygen, the Sr peak changes drastically in its shape and finally saturates with an exposure of 100 L. A remarkable effect on oxygen adsorption is that the relatively broad peak for the metallic surface is separated clearly into three peaks, denoted *A*, *B*, and *C* in Fig. 4(b). As will be shown explicitly later, none of peaks *A*, *B*, and *C* are attributable to multiple scattering because of the fact that the energy difference between the three peaks is almost independent of E_0 over a wide range from 100 eV to 1 keV. Namely, peak *A*, appearing at an energy position of $E = 167$ eV, is ascribed to elastic single scattering, and peaks *B* and *C* are caused by inelastic single scattering, the energy difference between peaks *A* and *B* (peak *C*), Q_B (Q_C), being inelastic energy loss, which amounts to 8 eV (20 eV). Among the three peaks, peak *C* seems to be ascribed to reionization because it appears at about the same energy position as ionized He^0. Strictly speaking, however, it is possible that another inelastic process contribute to peak *C*, but details will be provided later. As regards peaks *A* and *B* in Fig. 4(b), it should be noted that the FWHM of elastic peak *A*, 5 eV, is about half that of the spectral peak at the metallic surface, 10 eV, and that while peak *B* is located about 6 eV below the original peak position for a metallic surface, peak *A* is located about 2.5 eV above it. This clearly indicates that an inelastic process other than reionization makes an important contribution to the spectrum for the metallic surface as a peak broadening and for the oxidized surface as an appearance of peak *B*.

In order to clarify the origin of these inelastic effects, the metallic Sr surface is exposed to chlorine as well. The resultant Sr peak shown in Fig. 4(c) is also composed of three peaks whose energy positions coincide with those at the oxidized surface, although the intensity of inelastic peaks relative to that of the elastic peak is considerably small. It is worth noting that the Cl peak is also composed of a triple peak similar to the Sr peak, and that the energy difference between peaks *A* and *B* agrees with Q_B of the Sr peak within an experimental error of ± 1 eV. These results imply that the appearance of peak *B* is correlated with change in the surface-electronic states due to formation of the compounds. Only if the surface is covered with an oxide or chloride of strontium with a thickness of a monolayer the He^+ spectrum is expected to have a characteristic of those compounds, because of its high surface sensitivity. Hence, the loss energy $Q_B = 8.5$ eV is thought to be caused by a certain electronic excitation characteristic of SrO or $SrCl_2$. Actually, the He^+ spectrum from a thin film of $SrCl_2$ is confirmed to be the same as the spectrum in Fig. 4(c). Since these ionic compounds have a large band-gap energy, E_g, it is probable that Q_B corresponds to a certain branch of the interband excitation; E_g is known to be 7.3 eV for $SrCl_2$ and 6.4 eV for SrO. The discrepancy of Q_B from E_g, 1–2 eV, is not so serious because E_g, or an exitonic level measured from a top of the valence band, provides only a minimum energy of the electronic transition. If the energy resolution was sufficiently high, further information on the excited states could be obtained from the scattered-ion spectra. In order to confirm that the

present inelastic process is certainly caused by the band effect, energy spectra of He^+ scattered from several ionic crystals have been examined and the results are shown in the following three subsections. Before proceeding, we would like to show the data obtained from the $SrF_2(111)$ surface in the following.

Although the Q_B value for SrO coincides with that for $SrCl_2$, the loss value should be dependent on the band-gap energy E_g if peak B is definitely due to the band effect. Figure 5 shows energy spectra of He^+ scattered from each element of the $SrF_2(111)$ surface obtained by using a He^+ beam (solid curve) as well as a He^0 beam (dotted curve) with a kinetic energy E_0 ranging from 200 to 1000 eV under the conditions of $\alpha=80°$ and $\theta_L=160°$, the spectra being shown as a function of the loss energy Q from the BCE of Sr, $E_1=0.84E_0$, or of F, $E_1=0.44E_0$. It is found that the spectral peaks from Sr and F obtained

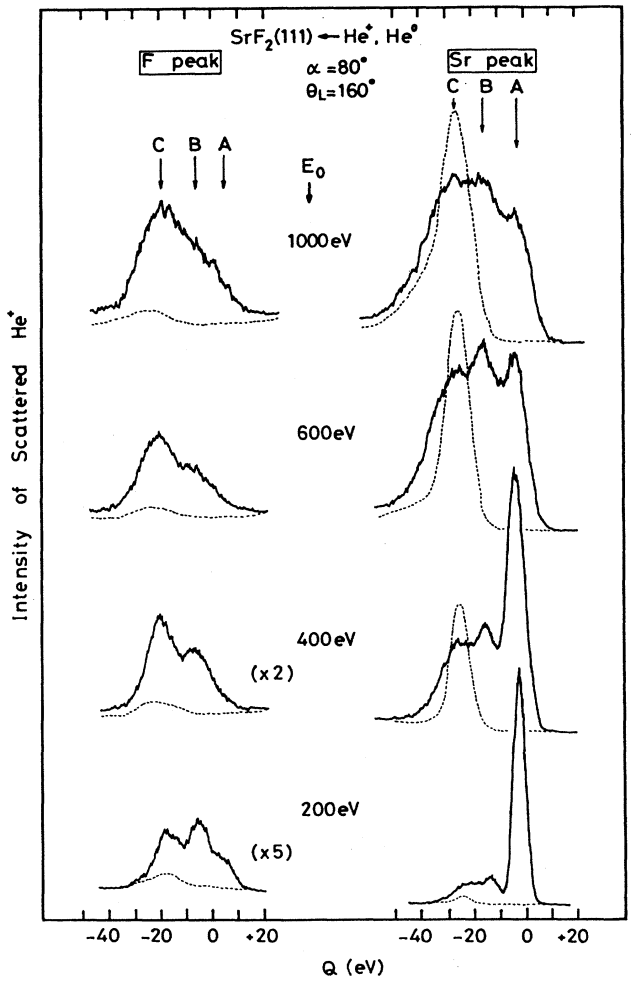

FIG. 5. The He^+ energy spectra from F and Sr ions at the $SrF_2(111)$ surface in the primary beam energy ranging from 200 to 1000 eV measured under the scattering condition of $\alpha=80°$ and $\theta_L=160°$; the normalized spectra by He^0 incidence (dotted curves) as well as He^+ incidence (solid curves) are shown as a function of the loss energy Q from BCE for each element.

by He^+ incidence are also composed of three peaks A, B, and C and that the loss peaks B and C increase in intensity relative to peak A with increasing kinetic energy. Peak C for Sr, corresponding well to a spectrum of ionized He^0, has been clearly observed even at the metallic Sr surface or surfaces of other Sr compounds, while peak B for Sr should be attributed to the electronic excitation characteristic of SrF_2 because of the fact that the loss value Q_B, which is measured to be 11 ± 0.5 eV, corresponds well to the band-gap energy E_g of SrF_2, 10.5 eV. The Q_B value for F also corresponds well to E_g. It is thus confirmed that peak B is caused by the He^+ ions that excite the valence electron (the anion p electron) to the conduction band (the s or d orbital of the cation) in the course of scattering.

With regard to the F peak, it should be noted that peak C exceeds the elastic peak A as well as peak B, even at such a small kinetic energy of 400 eV. One may think that peak C for F can be ascribed to reionization of He^0, but this assumption is discarded as follows: The reionization contribution to the spectral peak can be estimated by comparing the normalized He^+ spectrum by He^0 incidence with that by He^+ incidence since the former offers a maximal intensity of reionized He^0 included in the latter.[26] As we see in Fig. 5, peak C for F, being located at about the same energy position as the normalized spectra of ionized He^0, cannot be explained only as reionized He^0 since the intensity of ionized He^0 is rather small compared with that of peak C. Similar to this, peak C for Sr exceeds ionized He^0 in intensity, especially for a small kinetic energy as shown in Figs. 4 and 5, which strongly suggests that it cannot be ascribed only to reionization either. The origin of this inelastic scattering will be discussed later.

Here we would like to emphasize that the comparison of the normalized intensities between ionized He^0 and the loss peaks in the He^+ spectra directly offers the probability of Auger neutralization or resonance neutralization followed by Auger deexcitation on the incoming trajectory of the ions, provided no inelastic process other than reionization takes place.[29]

2. $CaF_2(111)$

Figure 6 shows normalized energy spectra of He^+ from the $CaF_2(111)$ surface obtained by using (a) He^+ and (b) He^0 beams of 200 eV at various glancing angles, α, in the $[10\bar{1}]$ azimuth, the scattering angle θ_L being fixed at 120°. The peak positions corresponding to ionized He^0 are also indicated by arrows on each spectrum in Fig. 6(a). In preliminary experiments on impact-collision ion-scattering spectroscopy (ICISS), it is known that the $CaF_2(111)$ surface is terminated by the F ions and has an unreconstructed 1×1 structure, as shown in the inset of Fig. 6, and that no shadowing of the Ca ions in the second layer by the first-layer F ions takes place in the $[10\bar{1}]$ azimuth.[30] The spectral peak from each component is composed of a triple peak similar to the results of the strontium halides. Peak B is confirmed to be caused by the interband electronic excitation due to the fact that the Q_B value, 11 eV, is in good agreement with the band-

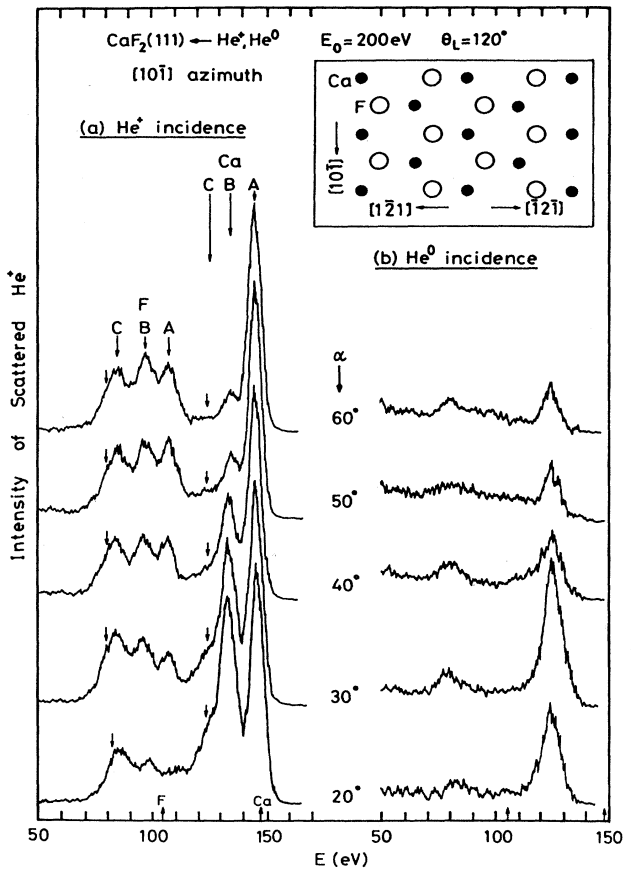

FIG. 6. Energy spectra of $E_0=200$ eV He^+ scattered from the $CaF_2(111)$ surface observed in the [10$\bar{1}$] azimuth at various glancing angles α with a fixed scattering angle $\theta_L=120°$. The spectra by (a) He^+ incidence and (b) He^0 incidence are normalized relative to each other through beam currents. The top view of the atomic arrangement of $CaF_2(111)$ is shown in the inset.

gap energy, 11.5 eV, and that peak B is not separated from peak A at metallic Ca surface.[24] The experimental result that peak C for Ca is reasonably small compared with the normalized spectral peak for ionized He^0, for a wide kinetic-energy range from 100 to 1000 eV, implies that it can be ascribed to reionization, while peak C for F exceeds ionized He^0 in intensity similar to that at $SrF_2(111)$ and should be attributable to other inelastic processes. The neutralization probability of He^+ due to the Auger process is thought to be small at the $CaF_2(111)$ surface because of the small intensity of reionized He^0 on Ca in comparison with that of ionized He^0, which can also be confirmed from the results that the intensity of peak A for Ca does not decrease for smaller α, for which the probability for the Auger neutralization is expected to be high.[16,18]

It should be emphasized that the intensity of peak B relative to that of peak A, I_B/I_A, strongly depends on the glancing angle for the Ca peak, but is weakly dependent on it for the F peak. A similar tendency is seen in the azimuthal-angle dependence of the peak intensities shown in Fig. 7 measured under the conditions of $\alpha=40°$ and $\theta_L=120°$. The I_B/I_A values for the Ca peak show a minimum in the [1$\bar{2}$1] azimuth and a maximum in the [$\bar{1}$2$\bar{1}$] azimuth, while those for the F peak are almost independent of the azimuthal angle. Since the band effect is essentially caused by excitation of a spatially localized F $2p$ electron to a rather extended conduction level, the probability of its occurrence is expected to be high if a collision occurs at a position close to the F ions. As we see in the inset of Fig. 6, indeed the turning point of He^+ off Ca is closer to the adjacent F ions in the [$\bar{1}$2$\bar{1}$] azimuth rather than the [1$\bar{2}$1] azimuth, which qualitatively explains the azimuthal-angle dependence of the I_B/I_A values for the Ca peak.

3. *Chlorides*

We measured energy spectra of He^+ from various kinds of chlorides in the kinetic-energy range below 300 eV so as to elucidate further information about the mechanism of the interband electronic transition. Most of the spectra explicitly shown in this section were measured at polycrystalline thin films evaporated on graphite in UHV, and the samples were confirmed to exhibit a clear band-gap energy in EELS after the ISS measurements. Figure 8 shows the energy spectra of He^+ from (a) NaCl

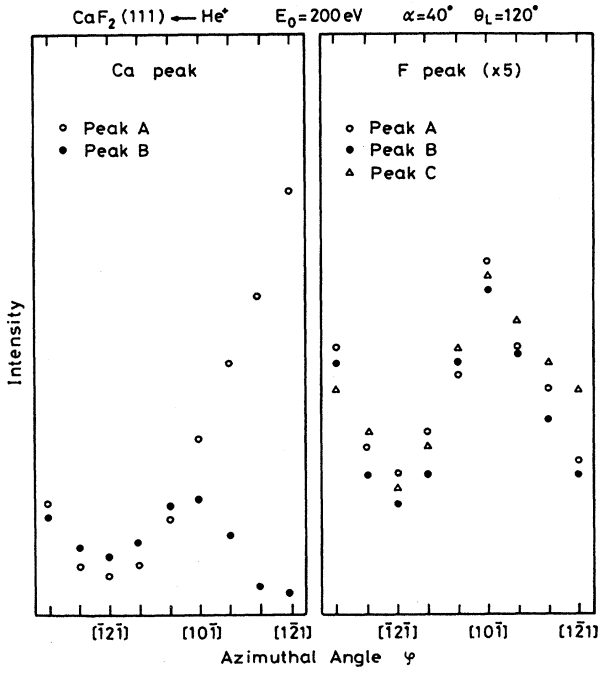

FIG. 7. Azimuthal-angle dependence of the partial intensities of the spectral peaks corresponding to (a) Ca and (b) F ions at the $CaF_2(111)$ surface. The measurements were made by using a He^+ beam of 200 eV under the conditions of $\alpha=40°$ and $\theta_L=120°$.

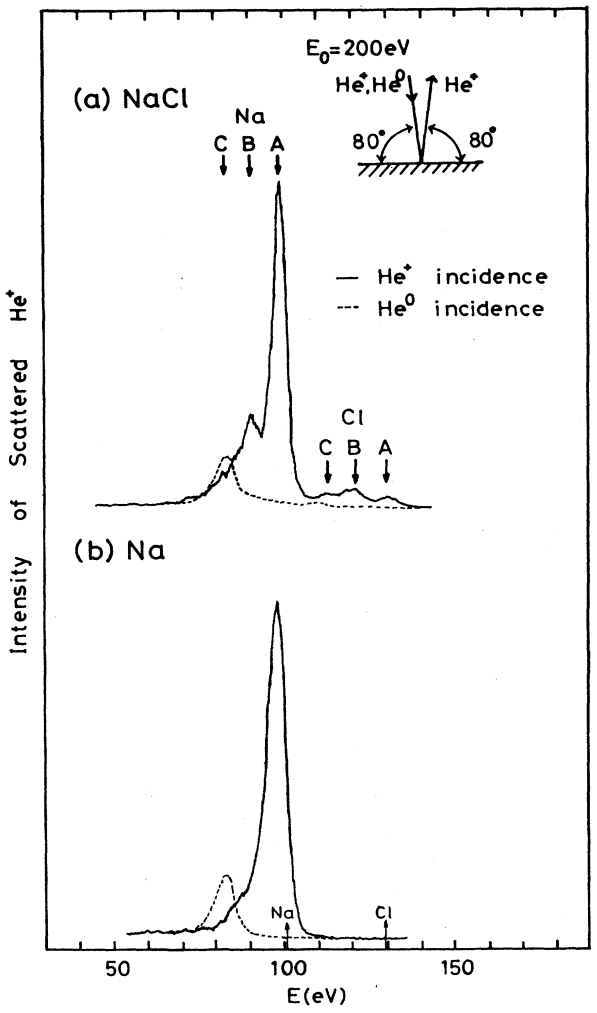

FIG. 8. Scattered He^+ spectra from polycrystalline thin films of (a) NaCl and (b) Na measured by using He^+ and He^0 beams of 200 eV under the condition shown in the inset. The spectra for He^0 incidence are normalized to those for He^+ incidence.

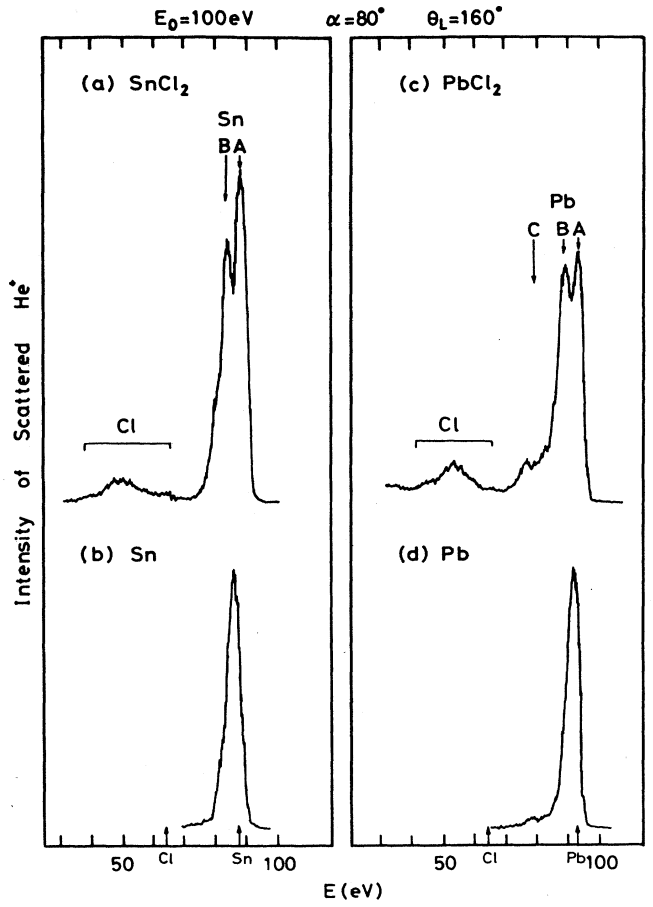

FIG. 9. Energy spectra of He^+ from (a) $SnCl_2$, (b) Sn, (c) $PbCl_2$, and (d) Pb by using a 100-eV He^+ beam under the same scattering conditions as Fig. 8.

and (b) Na obtained by using beams of He^+ and He^0 with a kinetic energy of 200 eV under the conditions shown in the inset. In Fig. 8(a) both Na and Cl peaks are composed of three components and peak B is easily ascribed to the interband electronic excitation since the Q_B value is in good agreement with $E_g = 8.5$ eV. Peak C for Na, which is small enough compared with the normalized spectrum of ionized He^0 shown by the dotted curve, can be ascribed to reionization, while peak C for Cl cannot be ascribed only to reionization as mentioned before. The measurements have also been made for the NaCl(100) surface; the spectra have the same features as Fig. 8(a) and the ratio I_B/I_A for the Na peak is found to be enhanced, especially for a small glancing angle in the [001] azimuth similar to the discussions concerning Figs. 6 and 7.

Figure 9 shows the energy spectra of He^+ from (a) $SnCl_2$, (b) Sn, (c) $PbCl_2$, and (d) Pb obtained by using a $E_0 = 100$ eV He^+ beam. The Sn peak as well as the Pb peak from a surface of each chloride is found to be accompanied by loss peak B due to the band effect, while the Cl peak is not clearly separated into the three peaks, in contrast to Fig. 8(a), because of a rather small band-gap energy of these chlorides, ~4 eV. The feature of the Pb peak is the appearance of peak C, which has already been reported by Shoji *et al.* for the metallic Pb surface.[31,32] It should be noted that reionized He^0 contributes very little to the Sn peaks as well as the Pb peaks shown in Fig. 9 since the probability for ionization of He^0 is estimated to be very small ($I^0/I^+ < 10^{-3}$) at $E_0 = 100$ eV. Hence, peak C for Pb, which is observed in the spectra of both $PbCl_2$ and Pb, should not be ascribed to reionization. It is known that Sn or Pb is a typical element that yields oscillations in the ion intensity versus the primary ion energy due to quasiresonant charge-exchange process.[15] Regarding the Pb peak for $PbCl_2$, indeed the oscillation is observed in the intensity of peak A in the energy range from 100 to 300 eV, while the intensity of peak B or C shows no oscillations in this energy range.

On the other hand, no oscillation is observed in the intensity of both peaks *A* and *B* for Sn at $SnCl_2$ in this energy region, but this is reasonable considering the data of Rusch and Erickson, in which very little oscillation takes place in the Sn-He^+ system for $E_0 < 300$ eV.[15]

Figure 10 shows energy spectra of He^+ from (a) CuCl and (b) $ZnCl_2$ obtained by using a He^+ beam of 100 and 200 eV respectively. In contrast to the cations explicitly shown in this paper, the Cu peak in CuCl and the Zn peak in $ZnCl_2$ are found to be composed only of peak *A* despite the fact that both surfaces have a clear band-gap energy that can be detectable under the present experimental conditions. In addition, the loss peak due to the band effect cannot detected in the Ag peak for AgCl either. The present result strongly suggests that occurrence of the interband electronic transition in the course of the He^+ scattering is also dependent on the species of target elements, or, in other words, the nature of the QM state during the collision.

4. *Other ionic compounds*

In the preceding subsections it is found that the inelastic scattering other than reionization or the electronic excitation beyond the band gap contributes to the spectra from F, Cl, Sr, and Pb. In this subsection we show examples of other elements that cause inelastic He^+ scattering unrelated to these two processes. Shown in Fig. 11 are the energy spectra of He^+ from (a) K, (b) KBr(100), and (c) KI obtained by using both He^+ and He^0 beams of 200 eV as well as 100 eV. Besides peak *B* due to the band effect, peak *C* is intensively observed in the K peak at an energy position about 18 eV below peak *A*, even at such a

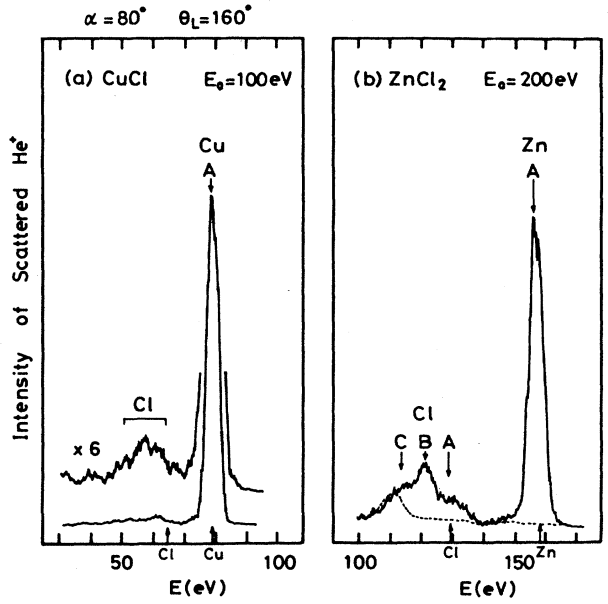

FIG. 10. Energy spectra of He^+ from (a) CuCl and (b) $ZnCl_2$ using a He^+ beam of 100 and 200 eV, respectively. The normalized spectrum by He^0 incidence is also shown by a dotted curve.

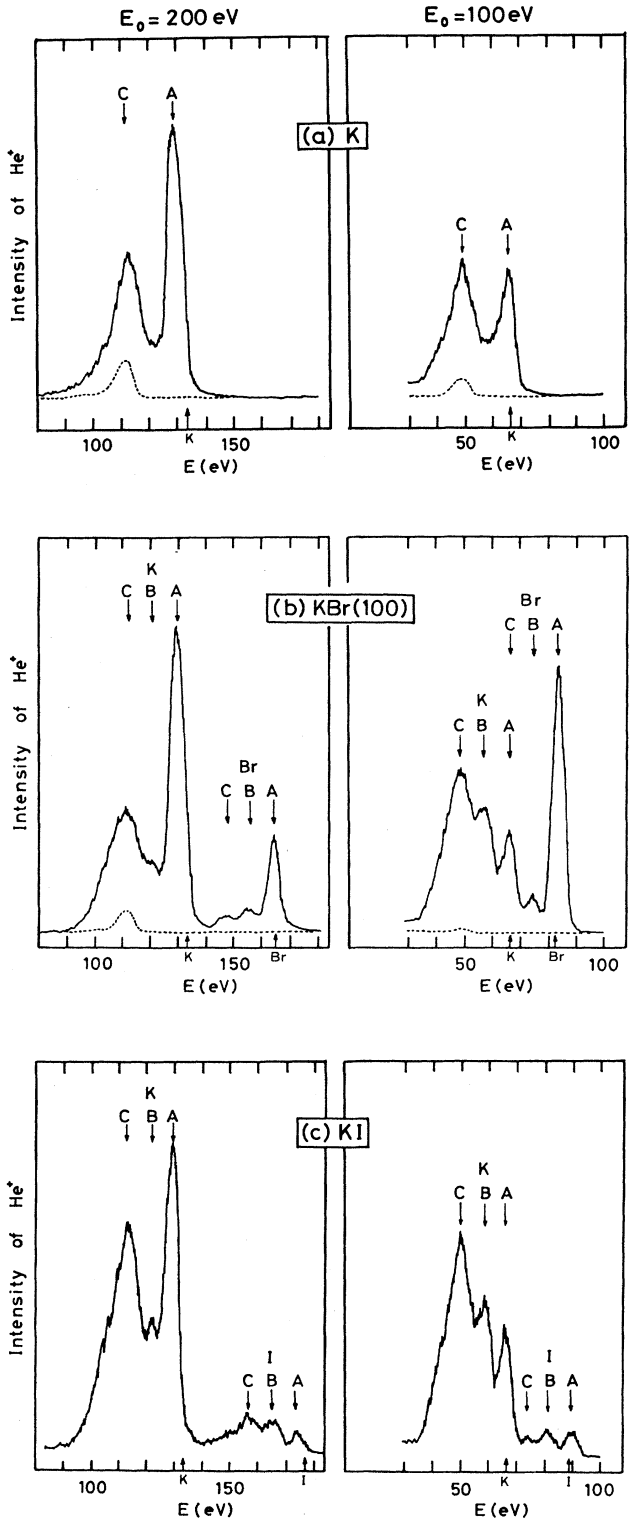

FIG. 11. Energy spectra of He^+ from (a) a metallic K surface, (b) the KBr(100) surface, and (c) a surface of polycrystalline KI obtained by using a beam of He^+ with a kinetic energy of 200 eV as well as 100 eV under the same scattering conditions as Fig. 8. The spectra from He^0 incidence are normalized in intensity and shown by dotted curves.

small kinetic energy as 100 eV, but cannot be ascribed to reionization because it is large enough compared with the normalized spectra of ionized He^0 shown by dotted curves. Since peak C is observed even in the spectrum from metallic K surface, it should be ascribed to a certain electronic excitation characteristic of the K atom. The Br and I peaks are also composed of three peaks, but peak C is not ascribed to reionization. The intensity ratio of the loss peak to the elastic peak increases with increasing the kinetic energy for all these spectral peaks for $E_0 > 300$ eV. Figure 12 shows the normalized K intensity for ionized He^0 relative to that for peak C (I^0/I_c^+) obtained at the metallic K surface as well as the KBr surface as a function of the kinetic energy E_0. The ratio, corresponding to the maximal contribution of reionization to loss peak C, is no more than 0.5 for $E_0 < 1$ keV and decreases with decrease of the kinetic energy. The result that the value for KBr decreases rapidly compared with that for metallic K may stem from the existence of the band gap in KBr.

Figure 13 shows energy spectra from RbCl obtained by using a He^+ beam (solid curve) as well as a He^0 beam (dotted curve) with a kinetic energy of (a) 300 eV and (b) 500 eV. A remarkable feature of the spectral peak is the contribution of additional peak C' to the Rb peak, which results in a rather broad loss peak typically seen in Fig. 13(b). Peak B due to the band effect cannot be separated from peak C for Rb in this energy region because the latter is large enough compared with the former. Comparing the normalized spectra of ionized He^0 with the loss peaks, we can conclude that neither of peaks C and C' for Rb is ascribed to reionization. It should be noted that the loss energy of ionized He^0 on Rb ($Q = 32$ eV) is rather large compared to that of peak C for Rb ($Q_c = 17$ eV). In addition to these alkali-metal halides explicitly shown here, the spectra from Cs at CsCl and Ba at $BaCl_2$ also include the loss peaks due to other than reionization, and the loss energies are measured to be 14 and 18 eV, respectively.

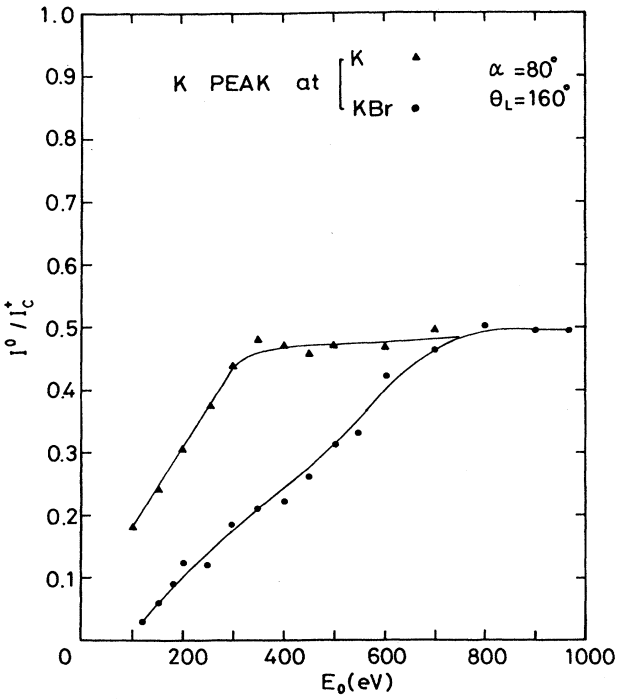

FIG. 12. Intensity ratio of ionized He^0 to peak C, I^0/I_c^+, corresponding to the K peak at a metallic K surface as well as a surface of KBr as a function of the primary beam energy.

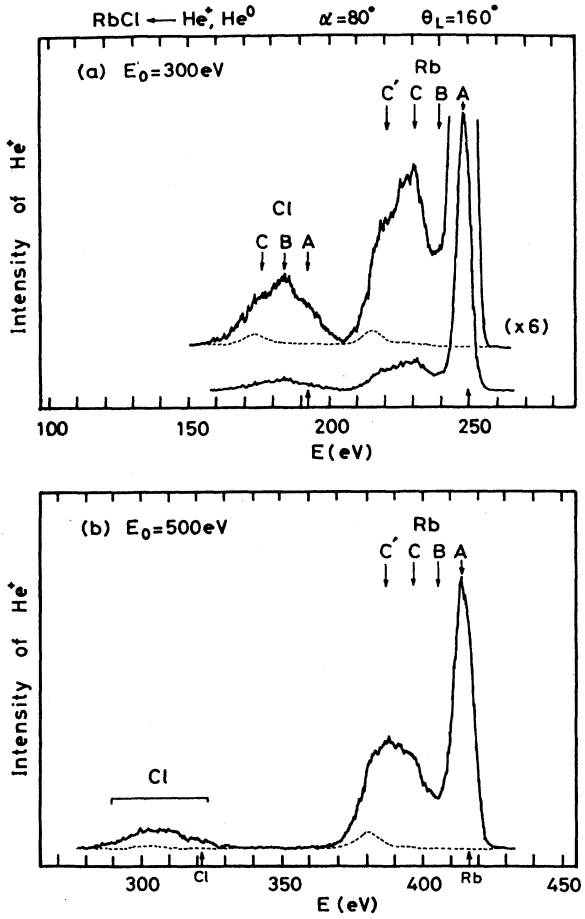

FIG. 13. Energy spectra of He^+ scattered from a polycrystalline thin film of RbCl measured by using both He^+ and He^0 beams of (a) 300 eV and (b) 500 eV. The spectra from He^0 incidence shown by dotted curves are normalized in intensity relative to those from He^+ incidence through beam currents.

IV. DISCUSSION

The points of the new findings in the preceding sections are summarized as follows.

(1) The promotion of the He 1s orbital in the QM state, which has been estimated from ionization of He^0, is suppressed if the target atoms have almost filled d orbitals in the energy position shallower than He 1s.

(2) The inelastic He^+ scattering due to interband electronic excitation takes place in the He^+ spectra from

Na^+ (NaCl), Mg^{2+} (MgF_2), K^+ (KBr, KI), Ca^{2+} (CaF_2), Rb^+ (RbCl), Sr^{2+} (SrF_2, $SrCl_2$, SrO), Sn^{2+} ($SnCl_2$), Cs^+ (CsCl), Ba^{2+} ($BaCl_2$), and Pb^{2+} ($PbCl_2$), as well as halogen ions, but it cannot be detected in the spectra from Cu^+ (CuCl), Zn^{2+} ($ZnCl_2$), and Ag^+ (AgCl), despite the fact that these compounds have a clear band-gap energy.

(3) The inelastic He^+ scattering, which is not ascribed to reionization or the electronic excitation beyond the band gap, makes an important contribution to the He^+ spectra from K, Rb, Cs, Ba, Pb, and halogen ions.

(4) Although the elastic He^+ scattering from Pb^{2+} at $PbCl_2$ yields oscillations in intensity of He^+ against primary ion energy due to the quasiresonant charge-exchange process, inelastically scattered He^+ shows no intensity oscillations against the kinetic energy.

According to the molecular-orbital (MO) calculations of Tsuneyuki and Tsukada, ionization of He^0 can be discussed on the basis of the diabatic electronic transition through crossing points of calculated adiabatic MO's, and the promotion of MO's correlated with the He 1*s* level, which is caused by the interaction of the He 1*s* orbital with the target core orbitals, is essential for ionization of He^0;[20,33] that is, as shown schematically in Fig. 14, the promoted He 1*s* orbital with the characteristic of the σ state necessarily interacts with above-lying valence orbitals, and then σ orbitals correlated with surface valence levels are promoted because crossing of MO's with the same symmetry is strongly avoided ("antibonding interaction"). At the interaction region, a crossing ("pseudocrossing") of the σ orbitals takes place as indicated by dashed curves, so that the He 1*s* electron can be promoted diabatically through the crossing point. The promotion results in ionization of He^0 if the He 1*s* electron is finally transferred to a vacant surface level.

As indicated in Sec. III A, the behavior of the He 1*s* orbital in the QM state is affected by specific electronic levels of the target atoms in the kinetic-energy region below 1 keV: The He 1*s* orbital may interact with the target *d* orbital so strongly that the promotion of the He 1*s* orbital shown in Fig. 14 is minimized if the target atom has filled *d* levels located in the energy position shallower than He 1*s*. Regarding the *s* or *p* orbital of the target, on the other hand, no effect on suppression of the He 1*s* orbital is seen in Fig. 3. One may think that the energetically localized nature of the *d* orbitals compared with the *sp* orbitals is responsible for the strong correlation with the He 1*s* orbital in the QM state, but this assumption is discarded as follows; a further measurement of the I^0/I^+ values similar to Fig. 3 is made for target elements with a 4*f* state that have a more localized nature than the *d* orbitals. For Pr (PrF_3), Lu (LuF_3), Hf (HfC), and Ta (TaC), the I^0/I^+ values are measured to be 0.53, 0.52, 0.24, and 0.27, respectively. Although Lu and Hf have a filled 4*f* level with a binding energy smaller than that of the He 1*s* orbital (7 eV for Lu and 18 eV for Hf), the I^0/I^+ values for these elements are almost comparable to those for Cs and Ba, which have no 4*f* states. (It should be noted that a ~4-eV work function should be added to the binding energy to refer the energy position from the vacuum level.) Thus the localized nature of the valence levels is found to be unrelated to the preferential correlation with the He 1*s* orbital. The present discussion strongly suggests that the orbital symmetry between the target-atom state and the ionic state is essential for description of the

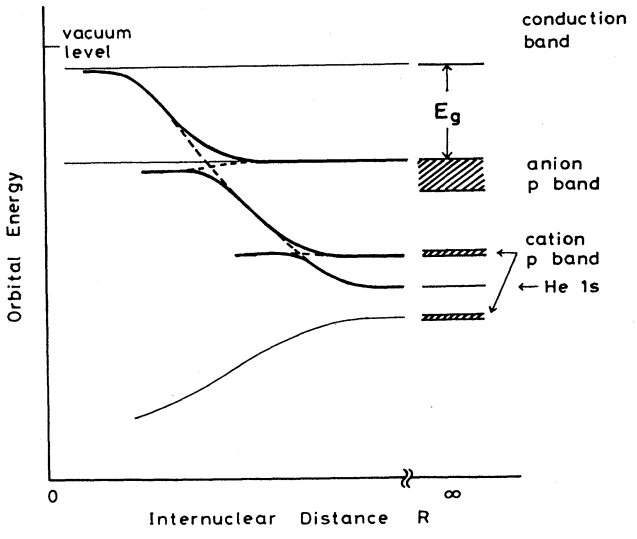

FIG. 14. Schematic diagram of molecular orbitals suitable for discussion of the inelastic He^+ scattering together with the surface band structure of ionic crystals in the separated-atom limit $R = \infty$. The promotion of the He 1*s* orbital in the QM state triggers successive promotion of the σ orbitals correlated with the surface bands due to the antibonding interaction. As a result, one or two electrons in the QM state can be transferred to the conduction band. (Re)ionization of He^0 is caused by the diabatic electronic transition shown by dashed curves.

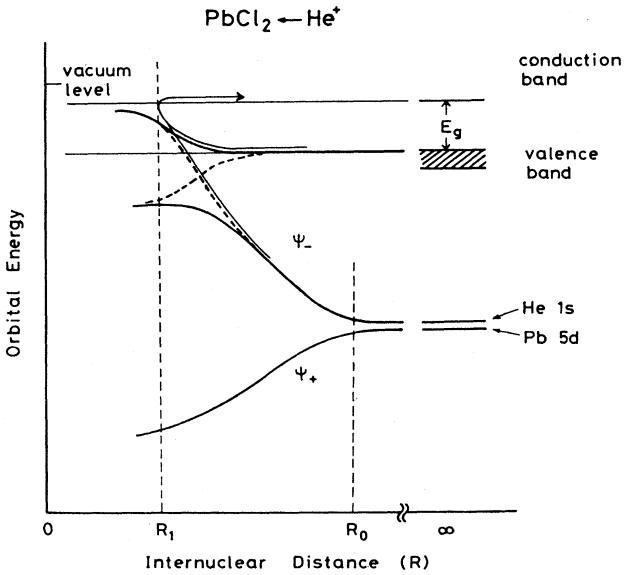

FIG. 15. Schematic view of QM energy levels responsible for the quasiresonant charge exchange as well as inelastic He^+ scattering.

QM state. The singularity in the correlation between He $1s$ and target d states has also been seen in the quasiresonant charge-exchange phenomema, in which the oscillatory yield curves of He^+ versus a primary beam energy are observed only if target atoms have energetically favorable d-electron states.[15]

The electronic excitation across the band gap is thought to be closely related to the QM state because its onset energy is strongly dependent on the sort of the target elements. If the excitation were caused by the dissipative force acting on the ion from a surface, the loss spectra would exhibit the electronic transition or the collective electronic motion given by the dielectric response function.[34] This is probably because the ionic motion in the present energy region is slow enough compared with the surface-electronic motion. In addition, the contribution of the electronic excitation through an excited $2s$ or $2p$ level of He^+, which is located energetically between the valence band and the conduction band, is thought to be marginal as well because the target-material dependence cannot be explained by this mechanism. Peak B for the target elements explicitly shown here has a clear onset energy below 100 eV and some of them are in good agreement with the calculated onset energies of the MO crossings in diatomic systems.[35] However, it should be noted that the electronic excitation is quite sensitive to the chemical binding of a target because it is readily affected by the anions adjacent to the target cation. This implies that a simple description based on the diatomic molecular orbital should be extended to include the whole electronic states surrounding the target. As a probable mechanism of the interband electronic excitation, we have proposed the following model: As discussed in Fig. 14, the σ orbitals correlated with surface bands can be promoted in succession due to the antibonding interaction with the He $1s$ orbital and the diabatic electronic transition through crossing points results in (re)ionization. The charge-exchange process at the energy-level crossing point of discrete levels has been successfully discussed on the basis of the Landau-Zener model,[36] and the probability for the diabatic transition at the crossing point is given as[20]

$$P = \exp(-2\pi V^2/v\,\Delta F)\ , \tag{2}$$

where V is the interaction matrix element of the crossing levels, ΔF is the difference between the slope of the two orbitals at the crossing point, and v is the relative velocity of the He^+ ion and a target atom. Hence, the diabatic transition is expected to be high if the kinetic energy $(mv^2/2)$ or the radial coupling at the crossing point $(\Delta F/V^2)$ is large enough. Contrary to this, if the kinetic energy of He^+ is small enough, the electronic excitation during formation of the QM state becomes adiabatic as indicated by solid curves in Fig. 14. On the basis of the present discussion, it can be concluded that the interband electronic excitation is caused by the adiabatic transition of the anion p electron through the first crossing point with the promoted σ orbital. This assumption has been supported by the fact that the interband electronic excitation has not been observed in the spectra from Cu (CuCl), Zn ($ZnCl_2$), and Ag (AgCl), which yield very little promotion of the He $1s$ orbital in the QM state and that the probability for the interband electronic excitation relative to that for ionization of He^0 is enhanced with decrease of the kinetic energy, as typically seen in Fig. 11(b).

Peak C for cations, such as K, Rb, Cs, and Ba, can be ascribed to excitation of their p electrons from analogy with excitation of anion p electrons: The binding energies of the p electrons for K, Rb, Cs, and Ba, being 18, 15, 13, and 16 eV, respectively, are small enough compared with the He $1s$ orbital energy, 24.6 eV. Hence a cation p electron can be promoted adiabatically through the crossing point with the He $1s$ orbital, then it diabatically passes through the crossing point with anion p orbitals, and finally it is transferred to the conduction band. Actually, the observed inelastic energy loss Q_C corresponding to these cations is in good agreement with the binding energy of the p electrons within ± 2 eV. On the other hand, excitation of a cation p electron makes no contribution to inelastic He^+ scattering for Na at NaCl, Mg at MgF_2, and Ca at CaF_2 since the p-electron binding energies of these elements (31 eV for Na, 52 eV for Mg, and 26 eV for Ca) are large enough compared with the He $1s$ orbital energy. In the case of Sr, since the $4p$ level is located at about 22 eV below the vacuum level, the excitation of the $4p$ electron may take place. As indicated in Figs. 4 and 5, in fact, peak C for Sr exceeds ionized He^0 in intensity, especially for a kinetic energy as small as 200 eV, which may result from the He^+ ions scattered inelastically after exciting a $4p$ electron of strontium.

It should be noted that excitation of the surface p electrons mentioned above is usually accompanied by reionization, and that the probability for the former relative to that for the latter is dependent not only on the kinetic energy, as clearly shown in Fig. 12, but also on the species of the target elements. This may result from the crossing nature of the potential curves in the QM state. For example, excitation of a cation p electron (ECP) for K (KBr) and Rb (RbCl) exceeds ionization of He^0 (IHE) or excitation of an anion p electron (EAP) in the energy region below 1 keV. In the case of Cs (CsCl) and Ba ($BaCl_2$), EAP seems to be main process at $E_0 = 200$ eV, while for $E_0 > 500$ eV ECP increases rapidly and results in a main part of the loss peak. As for these target elements, the intensity for IHE does not exceed 50% of that for ECP, even at $E_0 = 1$ keV.

Regarding the spectral peaks from anions, peak C can be ascribed neither to reionization nor to the inelastic process mentioned above, since no levels with the binding energy comparable to Q_C exist for the corresponding halides. The experimental results that Q_C is about twice as large as Q_B strongly suggest that peak C for anions stems from the He^+ ions that excite two valence electrons to the conduction band simultaneously during a single collision. The fact that only a one- or two-electron transition from the valence band to the conduction band selectively takes place strongly supports the present model that the preferential promotion of the σ orbital having a capacity of two electrons is responsible for the inelastic scattering as shown in Fig. 14. It is expected from this discussion that inelastic scattering corresponding to

simultaneous excitation of two electrons in a certain combination between EAP, ECP, and IHE may take place. In fact, the loss peak that probably may be attributable to simultaneous occurrence of IHE and ECP can be observed in the spectra of ionized He^0 on K, although its intensity is fairly small. In addition, peak C' for Rb in Fig. 13 may come from a combination of ECP and EAP. A precise MO calculation including the surface band structure is required for a further discussion about assignment of the spectral peaks, as well as the possible mechanisms other than the He $1s$-orbital-induced excitation shown here.

The He^+ scattering from Pb at $PbCl_2$ is of special interest since the quasiresonant charge-exchange process takes place in addition to the inelastic scattering. Figure 15 shows a schematic view of the energy levels for the QM state between He^+ and $PbCl_2$ as a function of the internuclear separation R. At $R<R_0$, mixing of the He $1s$ orbital and the energetically close-lying Pb $5d$ orbital takes place due to the exchange interaction, and the QM state is well described by bonding (ψ_+) and antibonding (ψ_-) orbitals shown in the figure. In the QM state the antibonding orbital is promoted first, and then interacts with the valence levels, and finally a valence electron can be transferred to a conduction band. From the viewpoint of the diabatic transition shown by dashed curves in the figure, it is equivalent to saying that the electronic hole in the antibonding orbital is occupied by a valence electron at the crossing point and then it is transferred to the conduction band. Peak C for Pb, not being attributable to reionization as mentioned earlier, is thought to be caused by excitation of a Pb $5d$ electron along the antibonding molecular orbital. On the other hand, the ratio I^0/I^+ for Sn shown in Fig. 3 is rather large compared with the value for Pb, which is measured to be 0.01 at $E_0=1$ keV. In the case of Sn, therefore, (re)ionization of He^0 can also make a contribution to the inelastic scattering and is known to yield no intensity oscillations versus a beam energy.[37]

The oscillatory behavior of the elastic peak A is caused by the quantum-mechanical interference between the bonding and antibonding orbitals as follows:[37] For $R_1<R<R_0$ the eigenstates of the QM state can be represented by bonding and antibonding eigenfunctions. For simplification, we assume the eigenfunctions can be written as

$$\psi_+=(\phi_{1s}+\phi_{5d})/\sqrt{2},\quad \psi_-=(\phi_{1s}-\phi_{5d})/\sqrt{2}\ , \tag{3}$$

where ϕ_{1s} and ϕ_{5d} stand for atomic orbitals of He $1s$ and Pb $5d$, respectively. Following the perturbed stationary-state method,[38] we can write the wave function of the hole that can be exchanged between Pb and He as

$$\Phi(t)=C_+\psi_+\exp\left[-\frac{i}{\hbar}\int_{t_0}^{t}\varepsilon_+(t)dt\right] +C_-\psi_-\exp\left[-\frac{i}{\hbar}\int_{t_0}^{t}\varepsilon_-(t)dt\right], \tag{4}$$

where $\varepsilon_+(t)$ and $\varepsilon_-(t)$ are energies of the bonding and antibonding orbitals. t_0 is the time when the observation is performed to specify the state to be $\Phi=C_+\psi_++C_-\psi_-$. In the case of the elastic He^+ scattering, t_0 is the time well before He^+ reaches the region $R=R_0$, and the initial condition for that time is given as $\Phi(t_0)=\phi_{1s}$, namely $C_+=C_-=1/\sqrt{2}$. Hence the survival probability for the quasiresonant neutralization is

$$P_Q=|\langle\phi_{1s}|\Phi(t_1)\rangle|^2=\cos^2\left[\frac{1}{2\hbar}\int_{t_0}^{t_1}\Delta\varepsilon(t)dt\right], \tag{5}$$

where $\Delta\varepsilon$ is defined as $\varepsilon_--\varepsilon_+$. This offers the oscillatory behavior of the intensity of peak A versus the kinetic energy.

For inelastic scattering, on the other hand, the coherence of the phase factors in Eq. (4) is broken down by the occurrence of the inelastic process at $R=R_1$, and hence we take t_0 as the time when the electronic excitation take place at $R=R_1$. The initial state at the time t_0 is given in this case as $\Phi(t_0)=\psi_-$, namely $C_+=0$ and $C_-=1$. Then the survival probability results in a constant, given as $P_Q=\frac{1}{2}$. It is thus concluded that the electron transfer, not from the atomic orbital of He or Pb, but from the antibonding molecular orbital of the Pb-He complex, is responsible for inelastic He^+ scattering, and that the quantum-mechanical interference effect is broken down by the intervening occurrence of a diabatic transition.

V. CONCLUSIONS

Electronic excitation and charge-exchange processes in impact scattering of He^+ from various solid surfaces have been investigated in the kinetic-energy range below 1 keV. A novel finding in the present work is excitation of surface valence electrons, which is usually accompanied by reionization of He^0. The probability for ionization of He^0 is minimized if target atoms have filled d levels located in an energy position shallower than the He $1s$ level. In He^+ scattering from ionic compounds, excitation of one or two electrons from the surface p bands to the conduction band has been observed, provided the p bands are located at an energy position shallower than the He $1s$ level, and provided the excitation of the He $1s$ electron sufficiently takes place. The main features of these experimental observations have been explained on the basis of the extended version of the quasimolecular framework: It is concluded that promotion of the molecular orbitals with a σ symmetry triggered by the excitation of the He $1s$ orbital is responsible for the inelastic He^+ scattering. The excitation of the surface p electrons, therefore, may take place due to the adiabatic transition of an electron at the first crossing point with the He $1s$ orbital, followed by the diabatic transitions at the crossing points with the molecular orbitals in a shallow energy position, while (re)ionization of He^0 is caused by a sequence of diabatic transitions. At lower energies, col-

lisions become adiabatic and, hence, excitation of the p electrons exceeds (re)ionization in probability. The diabatic transitions between the molecular orbitals also account for the breakdown of coherence in the quasiresonant charge-exchange process.

ACKNOWLEDGMENTS

We wish to thank Professor M. Aono, Professor M. Tsukada, Dr. S. Tsuneyuki, and Professor Y. Muda for fruitful discussions.

[1]D. P. Smith, J. Appl. Phys. **38**, 340 (1967).
[2]E. Taglauer and W. Heiland, Appl. Phys. **9**, 261 (1976).
[3]M. Aono, Nucl. Instrum. Methods B **2**, 374 (1984).
[4]S. H. Overbury, Surf. Sci. **112**, 23 (1981).
[5]H. Niehus, Surf. Sci. **166**, L107 (1986).
[6]M. Hou, W. Eckstein, and H. Verbeek, Radiat. Effects **39**, 107 (1978).
[7]P. Bertrand and M. Ghalim, Phys. Scr. T **6**, 168 (1983).
[8]F. Shoji and T. Hanawa, Nucl. Instrum. Methods B **2**, 401 (1984).
[9]S. H. A. Begemann and A. L. Boers, Surf. Sci. **30**, 134 (1972).
[10]W. Heiland, H. G. Schäffler, and E. Taglauer, Surf. Sci. **35**, 381 (1973).
[11]W. L. Baun, Phys. Rev. A **17**, 849 (1978).
[12]R. C. McCune, J. E. Chelgren, and M. A. Z. Wheeler, Surf. Sci. **84**, L515 (1979).
[13]M. Aono and R. Souda, Jpn. J. Appl. Phys. **24**, 1249 (1985).
[14]H. D. Hagstrum, Phys. Rev. **94**, 336 (1954).
[15]T. W. Rusch and R. L. Erickson, J. Vac. Sci. Technol. **13**, 374 (1976).
[16]R. Souda, M. Aono, C. Oshima, S. Otani, and Y. Ishizawa, Surf. Sci. **150**, L59 (1985); R. Souda and M. Aono, Nucl. Instrum. Methods B **15**, 114 (1986).
[17]R. Souda, M. Aono, C. Oshima, S. Otani, and Y. Ishizawa, Surf. Sci. **176**, 657 (1986).
[18]R. Souda, M. Aono, C. Oshima, S. Otani, and Y. Ishizawa, Surf. Sci. **179**, 199 (1987).
[19]M. Tsukada, S. Tsuneyuki, and N. Shima, Surf. Sci. **164**, L811 (1985).
[20]S. Tsuneyuki and M. Tsukada, Phys. Rev. **34**, 5758 (1986).
[21]S. Tsuneyuki, N. Shima, and M. Tsukada, Surf. Sci. **186**, 26 (1987).
[22]Y. Muda and D. M. Newns, Phys. Rev. B **37**, 7048 (1988).
[23]R. Souda, T. Aizawa, K. Miura, C. Oshima, S. Otani, and Y. Ishizawa, Nucl. Instrum. Methods B **33**, 374 (1988).
[24]R. Souda, T. Aizawa, C. Oshima, and Y. Ishizawa, Phys. Rev. Lett. **61**, 2705 (1988); Radiat. Effects (to be published).
[25]Th. Fauster, Vacuum **38**, 129 (1987).
[26]R. Souda, T. Aizawa, C. Oshima, S. Otani, and Y. Ishizawa, Surf. Sci. **194**, L119 (1988).
[27]M. Barat and W. Lichten, Phys. Rev. A **6**, 211 (1972).
[28]L. K. Verhey, B. Poersema, and A. L. Boers, Nucl. Instrum. Methods **132**, 565 (1976).
[29]R. Souda, T. Aizawa, C. Oshima, S. Otani, and Y. Ishizawa, Nucl. Instrum. Methods (to be published).
[30]R. Souda and M. Aono, in *Proceedings of the International Conference on the Structure of Surfaces, Amsterdam, 1987,* Vol. 11 of *Springer Series in Surface Science,* edited by J. F. van der Veen and M. A. Van Hove (Springer, New York, 1987), p. 581.
[31]F. Shoji, Y. Nakayama, and T. Hanawa, Surf. Sci. **163**, L745 (1985).
[32]F. Shoji, K. Oura, and T. Hanawa, Surf. Sci. **205**, L787 (1988).
[33]S. Tsuneyuki (private communication).
[34]R. Núñez, P. M. Echenique, and R. H. Ritchie, J. Phys. C **13**, 4229 (1980).
[35]R. Souda, T. Aizawa, C. Oshima, S. Otani, and Y. Ishizawa, Phys. Rev. B (to be published).
[36]E. E. Nikitin and S. Ya. Umanskii, *Theory of Slow Atomic Collisions* (Springer, Berlin, 1984).
[37]R. Souda, T. Aizawa, C. Oshima, M. Aono, S. Tsuneyuki, and M. Tsukada, Surf. Sci. **187**, L592 (1987).
[38]H. S. W. Massey and R. A. Smith, Proc. R. Soc. London, Ser. A **142**, 142 (1933).